Available online at www.eccomasproceedia.org
Eccomas Proceedia COMPDYN (2019) 5791-5801

ECCOMAS
Proceedia

COMPDYN 2019
7th ECCOMAS Thematic Conference on
Computational Methods in Structural Dynamics and Earthquake Engineering
M. Papadrakakis, M. Fragiadakis (eds.)
Crete, Greece, 24–26 June 2019

EFFECT OF ARCHITECTURAL NON-STRUCTURAL COMPONENTS ON LATERAL BEHAVIOUR OF CFS STRUCTURES: SHAKE-TABLE TESTS AND NUMERICAL MODELLING

Alessia Campiche[1] and **Sarmad Shakeel**[1]

[1] Department of Structures for Engineering and Architecture

University of Naples "Federico II", Naples; Italy
e-mail: alessia.campiche@unina.it

sarmad.shakeel@unina.it

Abstract

This paper illustrates the effect of architectural non-structural components on the variation of dynamic properties and lateral seismic behaviour of Cold-Formed steel (CFS) buildings, using shake-table tests and numerical modelling. The seismic behaviour of a two-storey gypsum-sheathed building was investigated as a part of European project ELISSA. Shake-table tests were carried-out on this building under two different configurations: with and without architectural non-structural components. Dynamic properties, such as fundamental period and damping ratio, of both building configurations were evaluated and compared. Numerical models considering all the architectural non-structural components were developed in Opensees environment. Results highlight the importance of considering the contribution of architectural non-structural components, such as finishing materials of shear and gravity walls, partition walls and internal counter walls, in the process of structural analysis and modelling of CFS buildings.

Keywords: CFS structures, Shake-table test, Non-Structural Components, OpenSees modelling.

Peer-review under responsibility of the organizing committee of COMPDYN 2019.
doi: 10.7712/120119.7345.19771

1 INTRODUCTION

Nowadays, Cold-Formed Steel (CFS) structures are often preferred to the traditional constructions as low-rise buildings in seismic areas due to their light weightiness and good seismic performance [1]. In fact, in the last decades numerous studies on elements [2–4], components [5–12] or whole buildings [13–15] have evaluated their seismic response. Although structural behaviour has been deeply investigated, only few experimental and numerical works have been carried out for the evaluation of the influence of architectural non-structural components on the global seismic response [16,17]. As demonstrated, the presence of non-structural architectural components offers a big contribution to the lateral resistance and stiffness of structure, but the current seismic design of CFS buildings does not take into account that contribution. To overcome this lack, as a part of European project ELISSA, the main task of University of Naples “Federico II” was the design and the execution of shake-table tests on full-scale two-storey CFS building in two different construction phases, which differ for the presence of architectural non-structural components. The influence of finishing material and other non-structural architectural components, i.e. partition walls and internal counter walls, on the dynamic properties of the structure (fundamental period of vibration and damping) has been evaluated, through the experimental results and numerical modelling. This paper summarises the experimental campaign and 3D building models developed in Opensees [18] software, focusing on the effect produced by non-structural architectural components on the seismic response.

2 EXPERIMENTAL CAMPAIGN

2.1 General

An experimental campaign aimed to deepen the knowledge of structural behaviour of CFS constructions, subjected to seismic excitations, was carried out at the Department of Structures for Engineering and Architecture of University of Naples “Federico II”. In particular, the influence of architectural non-structural components on the seismic behaviour was investigated through cyclic tests and shake-table tests. The cyclic tests were carried out on two full-scale gypsum-sheathed shear wall configurations, which differ only for the presence of finishing and insulating materials, whereas shake-table tests were carried out on a full-scale 3D building mock-up with and without architectural non-structural components. In particular, the wall specimen without finishing and insulating materials is named as B wall Configuration, while the specimen wall with finishing and insulating materials is named as C wall Configuration. Equally, the building mock-up without architectural non-structural components is named as B mock-up Configuration, while the building mock-up in which the architectural non-structural components were added is named as C mock-up Configuration. The B and C wall Configurations were representative of the shear walls used in the B and C mock-up Configurations, respectively. More details about the research project are available in Landolfo et al. [19].

2.2 Shear wall testing

The effect of the presence of finishing materials was evaluated through cyclic tests. The wall specimens had a dimension of 2.4 × 2.3 m (length x height). The two wall configurations are shown in Fig.1. The steel frame of specimens was mainly composed of intermediate and chord studs and tracks. The studs had 147×50×10×1.5 mm (outside-to-outside web depth × flange size × lip size × thickness) lipped channel (C) sections mainly spaced at 625 mm on the centre. Tracks had 150×40×1.5 mm (outside-to-outside web depth × flange size × thickness) unlipped channel (U) sections. All the steel members were made of S320GD+Z steel (characteristic yield strength: 320 MPa, characteristic ultimate tensile strength: 390 MPa). The steel frame was sheathed with 15.0 mm thick impact resistant gypsum board on both sides. In order to withstand the axial force due to overturning phenomena, back-to-back coupled studs and ad-hoc designed hold-down devices were placed at the wall ends. For the second test (C wall Configuration), the wall specimen was completed with insulation mineral wool, inserted among steel studs. The internal face was completed with an internal counter wall made of 20 mm thick vacuum insulated panel attached to the structural wall, 50×50×0.6 mm C vertical profiles spaced at about 600 mm, 50×40×0.6 mm U horizontal tracks, 50 mm thick insulation mineral wool. The steel frame of the internal counter wall was sheathed with double layer of 15 mm thick impact resistant gypsum board panels. The external face was completed with a ventilated façade made of a water proof membrane, 25×100 (outside-to-outside web depth × outside-to-outside flange size) slotted Ω horizontal profiles spaced at about 400 mm on the centre, sheathed with 12.5 mm thick cement-based outdoor board panels and finished with fibreglass mesh and cement plaster. Tests on wall specimens were conducted under displacement control in the reversed cyclic regime. The CUREE protocol, developed by Krawinkler et al. [20], was used.

Results are presented in the form of a comparison of cyclic behaviour obtained for the B and C Configurations walls (Fig. 2). Test results are shown in Table 1 in term of peak resistance per unit length (F_{max}/L), elastic resistance per unit length (F_e/L), which is the 40% of maximum resistance, drift corresponding to F_e (d_e/H), ultimate drift corresponding to a load equal to $0.80 \cdot F_{max}$ on the post-peak branch of the response curve (d_u/H) and conventional elastic stiffness per unit length (k_e/L) assumed equal to F_e / (L d_e). For both specimens the wall collapse was mainly governed by the tilting and pull-out of sheathing-to-frame connections. At global level, the steel frame deformed as a parallelogram with a consequent rigid rotation of the sheathing panels. In the case of C wall Configuration, the detachment of the sheathing panel, together with the wall lining of the internal face was also occurred for inter-storey drift ratios (IDR) higher than 4%. The presence of the finishing gave an increase in average of 48% for the wall strength and 39% for wall stiffness. Further details are available in Macillo et al. [21].

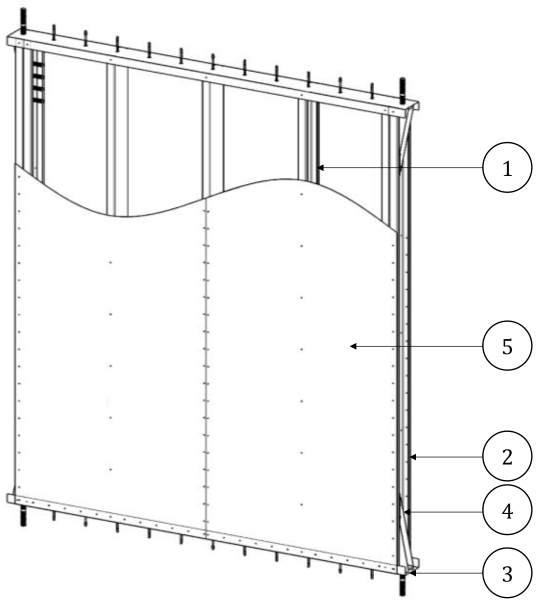

1. stud; 2. chord stud; 3. track; 4. hold-down; 5. gypsum board

a)

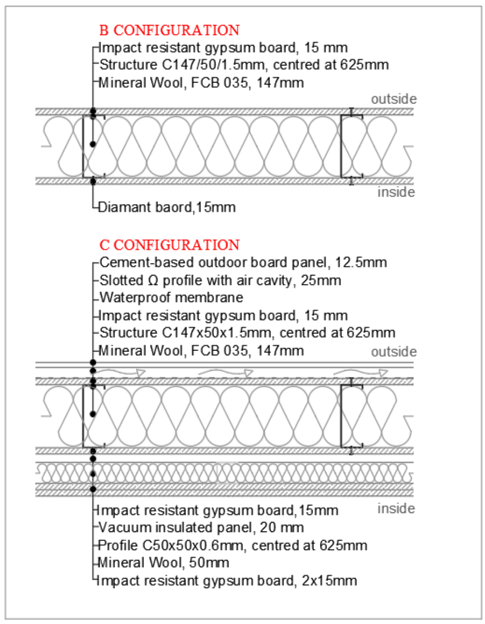

b)

Figure 1 a) View side of the B wall Configuration, b) Sections of B and C wall Configurations

Configuration		F_e/L [kN/m]	d_e/H [%]	k_e/L [kN/mm/m]	F_{max}/L [kN/m]	d_u/H [%]
B	Pos. Env.	5.60	0.19	1.28	14.00	1.97
	Neg. Env.	5.54	0.20	1.24	13.85	1.95
	Av.	5.57	0.19	1.26	13.92	1.96
C	Pos. Env.	8.47	0.23	1.63	21.17	2.71
	Neg. Env.	7.98	0.19	1.86	19.95	1.37
	Av.	8.22	0.21	1.75	20.56	2.04

Table 1 Cyclic test results of both B and C wall configurations

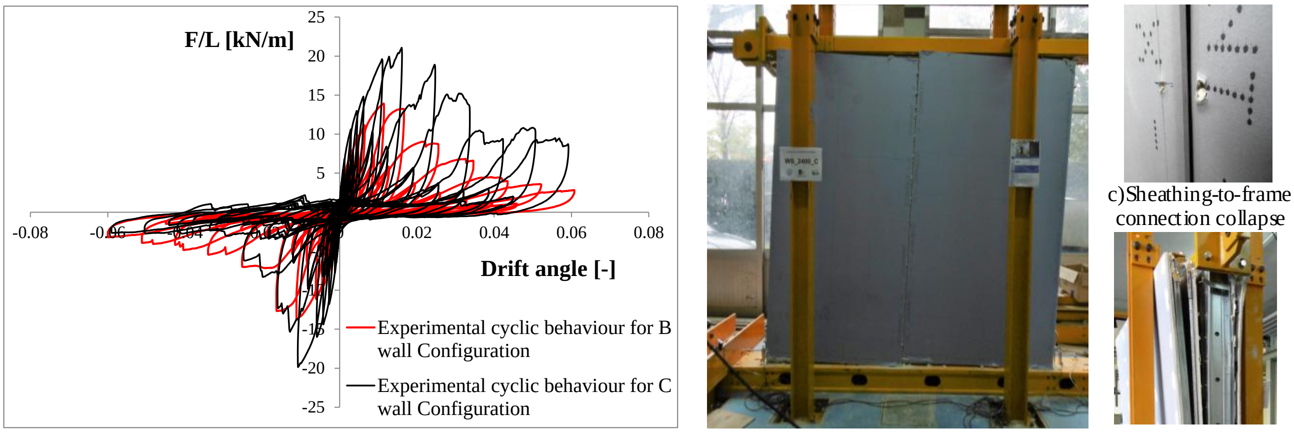

a) Experimental cyclic behaviours of B and C wall Configurations

b)Global deformation

c)Sheathing-to-frame connection collapse

d)Detachment of sheathing panel

Figure 2 Cyclic test results

2.3 Mock-up testing

A 3D building mock-up was tested on shaking table in two different construction phases: bare structure (B mock-up Configuration), consisting only of structural elements; and complete construction (C mock-up Configuration), in which architectural non-structural components were added. The mock-up was a 2.5×4.5×5.4 m (length x width x height) two storey building. The seismic resistant elements were made of CFS shear walls laterally braced by gypsum panels. A white noise signal was applied to the building (Random tests) in B and C Configurations in order to assess the main dynamic characteristics, i.e. first period of vibration and damping, while a natural ground motion record scaled by 5 to 150% (Earthquake tests) was applied only to C mock-up Configuration to evaluate its seismic response. Indeed, the experimental seismic response under an earthquake input is available only for the C mock-up Configuration.

The B mock-up Configuration consisted mainly of shear walls and gravity walls without finishing parts, internal partition walls, floors and roof. Shear walls had the same structure of the B wall Configuration tested under quasi-static cyclic regime (see Section 2.2). Gravity and partition walls had the same structural elements of shear walls. The main difference between shear and gravity walls was the presence of hold-down. In fact, in order to withstand the axial force due to overturning phenomena, ad hoc designed hold-down devices were placed only at the ends of shear walls. Internal partition walls, instead, were not designed to carry gravity loads. Floors and roof were made of back-to-back 197×50×10×2.0 mm C joists with a spacing of about 500 mm on the centre, connected at their end with 200×40×1.5 mm U floor tracks. The steel frame of the floors was sheathed on the top side with 28 mm thick high-density gypsum fibre board panels. The bottom side of steel frame of second floor and roof was sheathed with 15 mm thick impact resistant gypsum board panels.

The C mock-up Configuration was completed with architectural non-structural components, which mainly consisted of internal counter walls and finishing parts of shear walls, gravity walls, and finishing parts of floors and roof. In particular, shear walls had the same structure of the C wall Configuration tested under quasi-static cyclic regime and gravity walls were completed in the same way of the shear walls (see Section 2.2), however certainly without the hold down devices. Top sides of first and second floors were sheathed with additional gypsum fibre board panels, while bottom sides of second floor and roof were completed with a ceiling. The seismic weight of the B mock-up Configuration was evaluated to be approximately 24 kN for the second floor and 14 kN for the roof, while for the C mock-up Configuration they were approximately 50 kN and 26 kN, respectively. More details about mock-up are available in Fiorino et al. [22].

Random test results are presented in term of fundamental period of vibration and damping ratio for B and C mock-up Configurations, while the Earthquake test results are presented in term of peak and residual inter-storey drifts for C mock-up Configuration. The fundamental period for the B mock-up Configuration was greater than that recorded for the C mock-up Configuration. In particular, the fundamental period of the B mock-up Configuration was about 0.13 s, while for C mock-up Configuration it was about 0.10 s. As far as the measurement of damping ratio is concerned, it resulted in the range from 1.4% to 3.1% for the B mock-up Configuration and from 1.2% to 2.0% for the C mock-up Configuration. As concerned the peaks of the inter-storey drift ratio (PIDR) measured during earthquake tests carried out on the C mock-up Configuration, the PIDRs were 0.80% for 1st storey and 0.52% for 2nd storey. All the PIDRs corresponded to the earthquake with maximum intensity (scale factor equal to 150%). In addition, the residual inter-storey drift ratios (RIDRs) were very small (under 0.05%) and the observed damage was limited to architectural non-structural components, i.e. presence of gypsum dust and small detachment of cover paper at some corner joints on the inner faces of internal counter walls.

2.4 Effect of architectural non-structural components based on experimental results

Non-structural components explicitly considered in this study included insulating and finishing materials of shear and gravity walls, partition walls and internal counter walls. On the bases of experimental results, the effect of architectural non-structural components can be evaluated both on subsystem (shear wall) and whole building (mock-up). The evaluation of this effect for the shear walls can be done in term of stiffness, strength and collapse mechanisms, i.e. the cyclic tests on the shear walls were carried out up to the collapse on both shear walls without (B wall Configuration) and with architectural non-structural components (C wall Configuration). In contrast to shear walls, for the mock-up the effect of architectural non-structural components can be evaluated only in term of first period of vibration and stiffness, because the experimental seismic response under earthquake inputs is only available for mock-up with architectural non-structural components (C mock-up Configuration). Moreover, the partition walls are present in both B and C mock-up Configurations, therefore a rigorous comparison between B and C mock-up Configurations focused to assess the effect of non-structural components is affected by this circumstance. A further evaluation of the effect of architectural non-structural components was carried out through numerical modelling (see Section 3.6).

As experimental results showed, the increasing in stiffness due to the effect of non-structural components on the single shear wall was estimated equal to about 1.4 times, while the increasing in resistance was estimated equal to about 1.5 times, by comparing the lateral response of B and C wall Configurations. For the mock-up, the influence of non-structural components implied a global decreasing of the fundamental period of about 1.3 times from B to C mock-up configuration. Note that the variation of fundamental period of the mock-up was also affected by the variation of the mass, because the mass of the B mock-up Configuration was about one half than that of the C mock-up Configuration. Therefore, for the mock-up an increase of the estimated lateral stiffness equal to about 3 times can be associated to the decrease of the fundamental period. It is evident that the increase of lateral stiffness was greater for the mock-up than for the shear wall. This result confirms the important role of all architectural non-structural components, together with the box building behaviour, which increase significantly the lateral stiffness.

3 NUMERICAL MODELLING

3.1 General

Numerical models representative of B and C mock-up Configurations were developed in Opensees environment in order to capture their dynamic behaviour and seismic response. In particular, B Models are representative of the B mock-up Configuration and include shear walls (SW_B) and gravity walls (GW_B) without architectural non-structural components and partition walls, while C Models are representative of the C mock-up Configuration and include shear walls (SW_C) and gravity walls (GW_C) with non-structural finishing materials, partition walls (PW) and internal counter walls (ICW). Several modelling options were explored to deepen the knowledge of contribution offered by different structural and architectural non-structural components on the seismic response of the mock-up. They ranged from very simple models with only shear walls to more complex models, in which all the structural and architectural non-structural components were included. The effect of two different modelling choices for diaphragm was also evaluated. Diaphragm was either modelled as a rigid diaphragm constraint across all the nodes at floor or roof level, or as each joist (J) being modelled as a separate element without any constraint. Different modelling options are summarised in Table 2.

Mock-up Configuration	**Model**	**Structural***				**Non-structural***			
		SW_B	**IS**	**GW_B**	**J**	**PW**	**SW_C**	**GW_C**	**ICW**
B	**B1**	Yes	No	No	No	No	No	No	No
	B2	Yes	Yes	No	No	No	No	No	No
	B3	Yes	Yes	Yes	No	No	No	No	No
	B4	Yes	Yes	Yes	Yes	No	No	No	No
	B5	Yes	Yes	Yes	Yes	Yes	No	No	No
C	**C1**	Yes	Yes	Yes	Yes	Yes	Yes	No	No
	C2	Yes	Yes	Yes	Yes	Yes	Yes	Yes	No
	C3	Yes	Yes	Yes	Yes	Yes	Yes	Yes	Yes

*SW_B= shear wall without finishing materials, IS= intermediate studs, GW_B= gravity wall without finishing materials, J= floor joists, PW= partition walls, SW_C= shear wall with finishing materials, GW_C= gravity wall with finishing materials, ICW= internal counter wall

Table 2 Modelling options

3.2 Shear walls

The shear walls were modelled by a pair of diagonal trusses elements with a Pinching4 material, calibrated based on quasi static cyclic test response of the walls, as explained in the

Section 2.2. Pinching4 material is a material model, which represents a pinched load-deformation response and can exhibit degradation under cyclic loading, using the definition of the backbone envelope and the parameters governing the cyclic behaviour. In order to define the best-fit Pinching4 material for the shear walls, the force-displacement backbone curves assigned to diagonals were individuated first using the cyclic test results from the experiments, then the cyclic parameters were calibrated to best match the experimental response.

The shear wall models were subjected to the same loading protocol used in the cyclic tests. A parametrical analysis was performed to better match the cyclic behaviour of the walls through a quantitative comparison based on the energy dissipation per single cycle and cumulative cyclic energy. Figure 3 shows the comparison between experimental and numerical response in terms of load vs. displacement cyclic behaviour and cumulative dissipated energy. Hold-downs present at the ends of shear walls were modelled as ZeroLength elements with stiffness of 37kN/mm. The chord studs were modelled as truss elements with physical and mechanical properties representative of chord studs used in tested mock-up (147×50×1.5 mm C back-to-back sections), while the tracks were modelled as infinitely rigid truss elements. More details are available in Fiorino et al. [23]. Intermediate studs were neglected in the shear wall models as they are pin connected to their ends and do not contribute to the shear wall response.

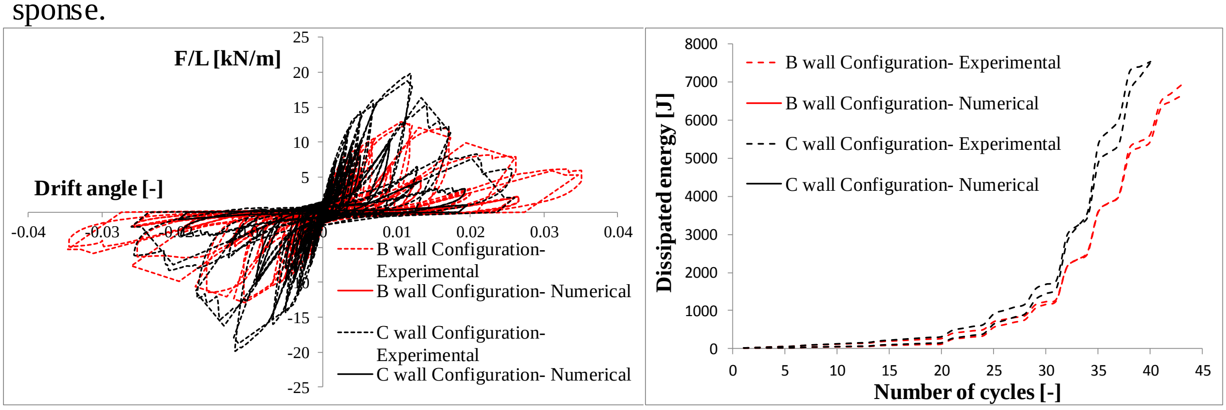

Figure 3: Experimental vs. numerical response in terms of load vs. displacement cyclic behaviour and cumulative dissipated energy

3.3 Other structural components

Apart from shear walls, other structural elements and components contribute to the seismic behaviour of the mock-up, i.e. intermediate studs, gravity walls, floors and roof. The intermediate studs were modelled as truss elements, with physical and mechanical properties representative of studs used in tested mock-up (147×50×1.5 mm C sections). The behaviour of gravity walls was also idealized as a pair of diagonal truss elements with Pinching4 material. The main difference between gravity and shear walls is the absence of hold-downs in gravity walls and the presence of hold down in shear walls. To reproduce the experimental rigid behaviour of the floors (ASCE 7-10), two different approaches were followed: rigid diaphragm or floor joists explicitly modelled. In the first approach the diaphragm was simulated by infinite rigid vertical and horizontal truss elements and in-plane X trusses applied at both floor intrados and extrados. In the second approach, joists were modelled as elastic beam column elements pin connected to the floor track elements, with the same properties of joists used in the mock-up (197×50×10×2.0 mm C back-to-back section. For further details see Campiche et al. [24].

3.4 Architectural non-structural components

Main architectural non-structural components present in the C mock-up Configuration were: finishing materials of shear walls and gravity walls, partition walls and internal counter walls. Finishing materials of shear and gravity walls were included directly in wall models, by using models representative of the walls with architectural non-structural components, i.e. model of shear wall with finishing materials (SW_C) and model of gravity wall with finishing materials (GW_C). The model of the partition walls was the same model used for the gravity walls. Since partition walls did not have present finishing materials, only test data of the B wall Configuration were used to calibrate the *Pinching4* material. The lateral force contribution provided by the double layer of impact resistant gypsum boards in counter walls was already lumped in the model of shear and gravity walls with finishing parts. Therefore, only the studs of internal counter walls were modelled as a truss element with their position in model and, the physical and mechanical properties being the representative of profiles used in tested mock-up (60×27×0.6 mm C sections). The end nodes of these studs were linked to the rigid truss elements of floors and they were constrained by the same rigid Diaphragm used to reproduce the rigid behaviour of the floor.

3.5 Numerical vs. Experimental response

In order to validate the numerical results, a comparison in term of dynamic properties (fundamental period of vibration) for B and C mock-up Configurations and seismic performance for C mock-up Configuration was performed. For each model, the fundamental period of vibration was evaluated via modal analysis (T_{NUM}) and was compared with the values evaluated on the bases of the experimental results (T_{EXP}), through the ratio $\Delta T = (T_{NUM} - T_{EXP})/T_{EXP}$ (Table 3) The models which gave the most accurate estimation of the fundamental period for the B and C mock-up Configurations were the B2 and C2 Models, respectively. They exhibited a fundamental period of vibration of about 0.12 s and 0.11 s, corresponding to a ΔT equal to about 3% and 7%, respectively.

For C Models, the peak inter-storey drifts were evaluated via non-linear time history analysis ($PIDR_{NUM}$) and were compared with the values obtained experimentally ($PIDR_{EXP}$), through the ratio $\Delta PIDR = (PIDR_{NUM} - PIDR_{EXP})/PIDR_{EXP}$. Moreover, experimental and numerical inter-storey drift time histories were compared. The model which gave the most accurate estimation of peak inter-storey drifts and better reproduced the experimental time history (Fig.4) was the C3 Model. It exhibited a PIDR equal to about 0.61% and 0.53% for the first and second storeys, corresponding to a ΔPIDR equal to about 24% and 2%, respectively.

Model	T_{NUM} [s]	T_{EXP} [s]	ΔT [%]
B1	0.143	0.130	13
B2	0.123		3
B3	0.118		7
B4	0.117		8
B5	0.100		21
C1	0.107	0.100	7
C2	0.095		5
C3	0.082		18

Table 3 Comparison between experimental and numerical fundamental period of vibration

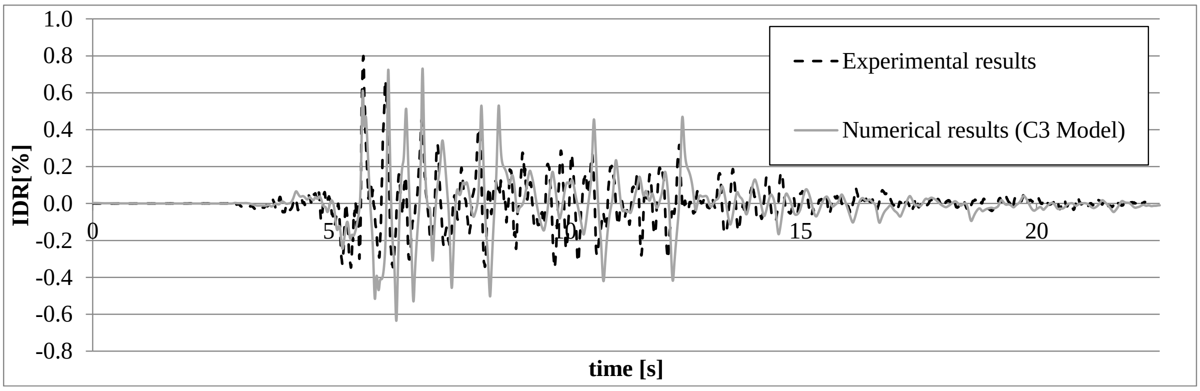

Figure 4: Comparison between experimental and numerical (C3 Model) IDR time history for the first storey

3.6 Effect of architectural non-structural components based on numerical results

Since the experimental data for the seismic response under earthquake input are not available for the B mock-up Configuration and partition walls were present in both B and C mock-up Configurations, the effect of architectural non-structural components on the seismic response of the mock-up was investigated numerically. The B4 Model, in which only all the structural components are modelled, and C3 Model, i.e. the model including all structural and non-structural components, were subjected to non-linear time history analysis and the results, in terms of IDR time history (Fig. 5), PIDR and residual inter-storey drift ratio (RIDR) were compared. PIDRs were 1.24% and 0.61%, while RIDRs were equal to 0.058% and 0.024% for B4 and C3 Models, respectively. The comparison of earthquake response of B4 and C3 Models shows the decreasing of the PIDR in C3 Model due to the effect of non-structural components on the whole building equal to about 2.0 times, while the decreasing of RIDR was estimated equal to about 2.4 times. Obviously, due to the non-linear response of the building under the earthquakes with higher intensity, the influence of the non-structural components in terms of PIDR reduction becomes lower in comparison with their effect on the increasing of initial lateral stiffness (see Section 2.4). However, also results in terms of earthquake response confirm the important role of all architectural non-structural components, which can significantly reduce peak and residual inter-storey drifts.

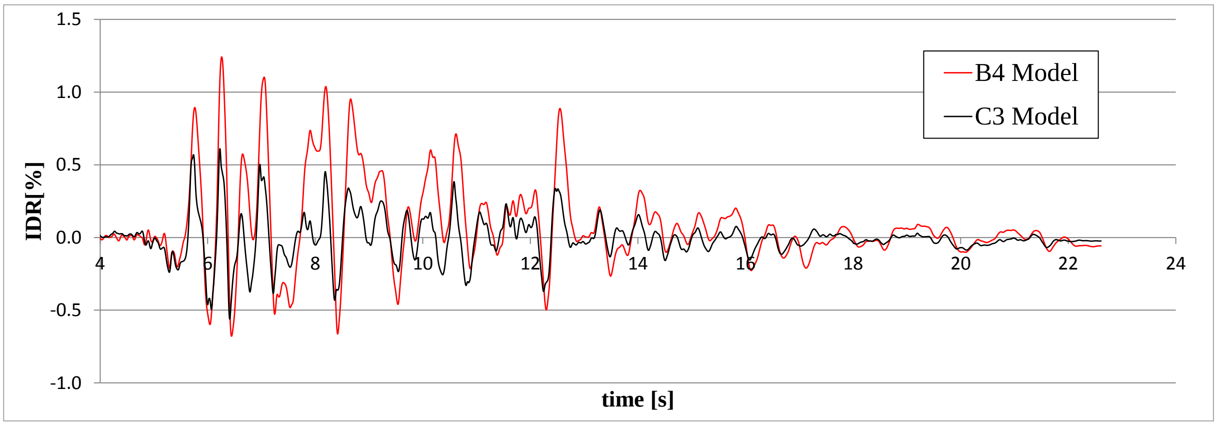

Figure 5: Inter-storey drift time history for B4 and C3 models

4 CONCLUSIONS

The present paper summarises the study on the effect of architectural non-structural components on the seismic behaviour of CFS structures, through the experimental test results and numerical modelling. Cyclic tests on full-scale gypsum sheathed shear walls with and without finishing materials and shake-table tests on full-scale two-storey CFS building with and without the architectural non-structural components and finishing materials were carried out. On the basis of the experimental results different numerical models of the building were developed in Opensees software, considering architectural non-structural components.

Based on the experimental results, the increasing in lateral stiffness and resistance due to the effect of non-structural components on the single shear wall was estimated equal to about 1.4 and 1.5 times, respectively; while for the building the effect of non-structural components, together with the box building behaviour, increased the lateral stiffness of about 3 times. Based on the numerical results, the decreasing of the inter-storey drift due to the effect of non-structural components was estimated equal to about 2.0 in terms of peak value and 2.4 times in terms of residual value.

Therefore, both experimental and numerical results confirm the important role of all architectural non-structural components, together with the box building behaviour, which significantly increase lateral stiffness and strength and reduce peak and residual inter-storey drifts.

REFERENCES

[1] R. Landolfo, Lightweight steel framed systems in seismic areas : Current achievements and future challenges, Thin-Walled Struct. 140 (2019) 114–131.

[2] L. Fiorino, V. Macillo, R. Landolfo, Experimental characterization of quick mechanical connecting systems for cold-formed steel structures, Adv. Struct. Eng. 20 (2017) 1098–1110. doi:10.1177/1369433216671318.

[3] L. Fiorino, T. Pali, B. Bucciero, V. Macillo, M. Teresa Terracciano, R. Landolfo, Experimental study on screwed connections for sheathed CFS structures with gypsum or cement based panels, Thin-Walled Struct. 116 (2017) 234–249. doi:10.1016/j.tws.2017.03.031.

[4] M.T. Terracciano, V. Macillo, T. Pali, B. Bucciero, L. Fiorino, R. Landolfo, Seismic design and performance of low energy dissipative CFS strap-braced stud walls, Bull. Earthq. Eng. 17 (2019) 1075–1098. doi:10.1007/s10518-018-0465-y.

[5] V. Macillo, O. Iuorio, M.T. Terracciano, L. Fiorino, R. Landolfo, Seismic response of Cfs strap-braced stud walls: Theoretical study, Thin-Walled Struct. 85 (2014) 301–312. doi:10.1016/j.tws.2014.09.006.

[6] L. Fiorino, O. Iuorio, V. Macillo, M.T. Terracciano, T. Pali, R. Landolfo, Seismic Design Method for CFS Diagonal Strap-Braced Stud Walls: Experimental Validation, J. Struct. Eng. 142 (2016) 04015154. doi:10.1061/(ASCE)ST.1943-541X.0001408.

[7] V. Macillo, S. Shakeel, L. Fiorino, R. Landolfo, Development and Calibration of a Hysteretic Model for CFS Strap braced stud walls, Adv. Steel Constr. 14 (2018) 337–360. doi: 10.18057/IJASC.2018.14.3.2

[8] L. Fiorino, M.T. Terracciano, R. Landolfo. Experimental investigation of seismic behaviour of low dissipative CFS strap-braced stud walls. J. Const. Steel Res. 127 (2016), pp. 92-107. doi:10.1016/j.jcsr.2016.07.027

[9] L. Fiorino, T. Pali, R. Landolfo, Out-of-plane seismic design by testing of non-structural lightweight steel drywall partition walls, Thin-Walled Struct. 130 (2018) 213–230. doi:10.1016/j.tws.2018.03.032.

[10] T. Pali, V. Macillo, M.T. Terracciano, B. Bucciero, L. Fiorino, R. Landolfo, In-plane quasi-static cyclic tests of nonstructural lightweight steel drywall partitions for seismic performance evaluation, Earthq. Eng. Struct. Dyn. 47 (2018) 1566–1588. doi:10.1002/eqe.3031.

[11] L. Fiorino, B. Bucciero, R. Landolfo, Evaluation of seismic dynamic behaviour of drywall partitions, façades and ceilings through shake table testing, Eng. Struct. 180 (2019) 103–123. doi:10.1016/j.engstruct.2018.11.028.
[12] R. Tartaglia, M. D'Aniello, G.A. Rassati, J.A. Swanson, R. Landolfo, Full strength extended stiffened end-plate joints: AISC vs recent European design criteria, Eng. Struct. 159 (2018) 155–171. doi:10.1016/j.engstruct.2017.12.053.
[13] L. Fiorino, O. Iuorio, R. Landolfo, Designing CFS structures: The new school bfs in naples, Thin-Walled Struct. 78 (2014) 37–47. doi:10.1016/j.tws.2013.12.008.
[14] L. Fiorino, S. Shakeel, V. Macillo, R. Landolfo, Behaviour factor (q) evaluation the CFS braced structures according to FEMA P695, J. Constr. Steel Res. 138 (2017) 324–339. doi:10.1016/j.jcsr.2017.07.014.
[15] R. Tartaglia, M. D'Aniello, A. De Martino, G. Di Lorenzo, Influence of EC8 rules on P-Delta effects on the design and response of steel MRF., Ing. Sismica Int. J. Earthq. Eng. 35 (2018) 104–1.
[16] V. Nikolaidou, C.A. Rogers, D.G. Lignos, Influence of Non-Structural Components on the Seismic Response of Cold - Formed Steel Structures, 3 (2017) 1–12.
[17] R. Montuori, E. Nastri, V. Piluso, Modelling of floor joists contribution to the lateral stiffness of RC buildings designed for gravity loads, Eng. Struct. 121 (2016) 85–96.
[18] S. Mazzoni, F. McKenna, M.H. Scott, G.L. Fenves, OpenSees, (2009).
[19] R. Landolfo, O. Iuorio, F. Luigi, Experimental seismic performance evaluation of modular lightweight steel buildings within the ELISSA project, Earthq. Eng. Struct. Dyn. (2018) 1–23. doi:10.1002/eqe.3114.
[20] H. Krawinkler, P. Francisco, L. Ibarra, A. Ayoub, R. Medina, CUREE publication No. W-02 Development of a Testing Protocol for Woodrame Structures, (2001).
[21] V. Macillo, L. Fiorino, R. Landolfo, Seismic response of CFS shear walls sheathed with nailed gypsum panels: Experimental tests, Thin-Walled Struct. 120 (2017) 161–171. doi:10.1016/j.tws.2017.08.022.
[22] L. Fiorino, V. Macillo, R. Landolfo, Shake table tests of a full-scale two-story sheathing-braced cold-formed steel building, Eng. Struct. 151 (2017) 633–647. doi:10.1016/j.engstruct.2017.08.056.
[23] L. Fiorino, S. Shakeel, V. Macillo, R. Landolfo, Seismic response of CFS shear walls sheathed with nailed gypsum panels: Numerical modelling, Thin-Walled Struct. 122 (2018) 359–370. doi:10.1016/j.tws.2017.10.028.
[24] A. Campiche, S. Shakeel, V. Macillo, M.T. Terracciano, B. Bucciero, T. Pali, L. Fiorino, R. Landolfo, Seismic Behaviour of Sheathed CFS Buildings: Shake Table Tests and Numerical Modelling, Ing. Sismica-International J. Earthq. Eng. 2 (2018) 106–123.